Molecular Crystals and Liquid Crystals
Publication details, including instructions for authors and subscription information:
http://www.tandfonline.com/loi/gmcl20

Formation and Reorganization of the Mesophase of Isotactic Polypropylene

Daniela Mileva [a], René Androsch [a], Evgeny Zhuravlev [b], Christoph Schick [b] & Bernhard Wunderlich [c]

[a] Martin-Luther-University Halle-Wittenberg, Center of Engineering Sciences, D-06099, Halle/Saale, Germany

[b] University of Rostock, Institute of Physics, D-18051, Rostock, Germany

[c] 200 Baltusrol Rd, Knoxville, TN, 379234-37-7, USA

Available online: 02 Mar 2012

To cite this article: Daniela Mileva, René Androsch, Evgeny Zhuravlev, Christoph Schick & Bernhard Wunderlich (2012): Formation and Reorganization of the Mesophase of Isotactic Polypropylene, Molecular Crystals and Liquid Crystals, 556:1, 74-83

To link to this article: http://dx.doi.org/10.1080/15421406.2012.635912

Mol. Cryst. Liq. Cryst., Vol. 556: pp. 74–83, 2012

ISSN: 1542-1406 print/1563-5287 online
DOI: 10.1080/15421406.2012.635912

Taylor & Francis
Taylor & Francis Group

Formation and Reorganization of the Mesophase of Isotactic Polypropylene

DANIELA MILEVA,[1] RENÉ ANDROSCH,[1,*]
EVGENY ZHURAVLEV,[2] CHRISTOPH SCHICK,[2]
AND BERNHARD WUNDERLICH[3]

[1]Martin-Luther-University Halle-Wittenberg, Center of Engineering Sciences, D-06099 Halle/Saale, Germany
[2]University of Rostock, Institute of Physics, D-18051 Rostock, Germany
[3]200 Baltusrol Rd, Knoxville, TN 379234-37-7, USA

A short review about the structure, condition of formation, and reorganization behavior of the mesophase of isotactic polypropylene, summarizing recent work of the authors, is provided. Emphasis is put on the presentation of data collected by novel analysis techniques like fast scanning chip calorimetry (FSC), temperature-resolved X-ray analysis, or temperature-resolved atomic force microscopy (AFM), for quantitative characterization of the kinetics of the liquid—mesophase transition and of the conversion of the mesophase into crystals. In addition, the impact of crystallization of polypropylene via intermediate formation of a mesophase on engineering properties will be highlighted.

Keywords Crystallization; isotactic polypropylene; mesophase; reorganization

Introduction

Isotactic polypropylene (iPP) belongs to the group of semicrystalline polymers, with the structure of the ordered phase depending on the conditions of crystallization [1]. Solidification of the quiescent melt of iPP may either lead to formation of monoclinic, lamellar α-crystals which coexist with amorphous structure within spherulites, or to formation of a mesophase [2–6]. The mesophase is of nodular shape [7,8] and is not arranged in a higher-order superstructure. In the α-phase, molecular segments adopt a 3_1 helix conformation, and left- and right-handed helices are parallel aligned within separate layers [9]. In the mesophase the helical structure of molecule segments is preserved, however, three-dimensional long-range order is lost due to presence of conformational defects like helix reversals or wrong inclination of the methyl groups of neighbored chains [10,11]. Both polymorphs yield characteristic X-ray patterns which allow straightforward identification.

For illustration of characteristic morphological features of semicrystalline and semimesomorphic iPP at different length scales, in Fig. 1 are shown microscopy images, collected by atomic force microscopy (AFM) (top row, Figs. 1a and 1b) and by polarizing optical microscopy (POM) (bottom row, Figs. 1c and 1d) [12]. The AFM patterns show the

*Address correspondence to René Androsch, Martin-Luther-University Halle-Wittenberg, Center of Engineering Sciences, D-06099 Halle/Saale, Germany. Phone: +49 3461 46 3762. Fax: +49 3461 46 3891. E-mail: rene.androsch@iw.uni-halle.de

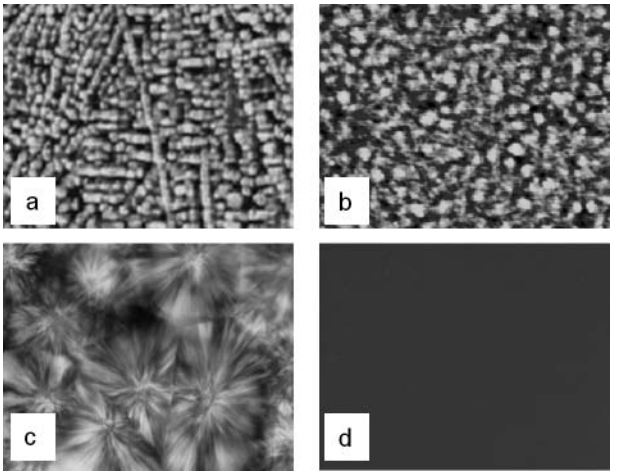

Figure 1. AFM images (top row) and POM images (bottom row) of semicrystalline (left) and semimesomorphic iPP (right). The AFM images show the structure at the nanometer length scale and the POM micrographs show the structure at the micrometer length scale. Adapted/Reprinted from Polymer, Vol. 50, D. Mileva, Q. Zia, R. Androsch, H.-J. Radusch, S. Piccarolo, "Mesophase formation in poly(propylene-*ran*-1-butene) by rapid cooling," pages 5482–5489, Copyright 2009, with permission from Elsevier.

structure at the nanometer length scale, while the POM images provide information about the superstructure at the micrometer length scale. Figures 1a and 1c were obtained on semicrystalline iPP and show lamellar crystals and spherulites, respectively, and Figs. 1b and 1d were obtained on semimesomorphic iPP and prove the particle-like habit of the mesophase and absence of spherulites, respectively. These morphological characteristics of the mesophase of iPP are in accord with a homogeneous nucleation mechanism, as will be demonstrated further on discussion of the temperature range of mesophase formation below.

Figure 2 is a summary of the conditions of mesophase formation in terms of temperature—time profiles [13]. The mesophase can be formed on cooling the quiescent melt or on heating the amorphous glass, as is indicated with the pathways C1/C2 and H1/H2, respectively. Details regarding rates of cooling and heating, or the exact temperature range of mesophase formation have been collected by fast scanning calorimetry (FSC) [14–17], or by investigation of the structure of samples of different thermal history [18,19]. Formation of the mesophase from the melt requires sufficiently fast quenching of the liquid in order to avoid crystallization in the temperature range between the equilibrium melting temperature $T_{m,0}$ of 460.7 K [20] and about 330 K. In addition, the cooling rate q must be lower than a critical value if the cooling step is performed to temperatures below the glass transition temperature T_g.

Crystallization of the melt is suppressed on cooling faster than about 10^2 K s^{-1}. The mesophase may then form on isothermal holding the supercooled liquid at a temperature between about 330 K and T_g (pathway C1). Alternatively, mesophase develops also on continued cooling below T_g if the cooling rate is lower than 10^3 K s^{-1} (pathway C2). Faster cooling inhibits both crystallization and mesophase formation and yields a fully amorphous glass. Mesophase formation occurs then on subsequent devitrification of the amorphous phase by heating above T_g (pathways H1 and H2). If the temperature range of mesophase

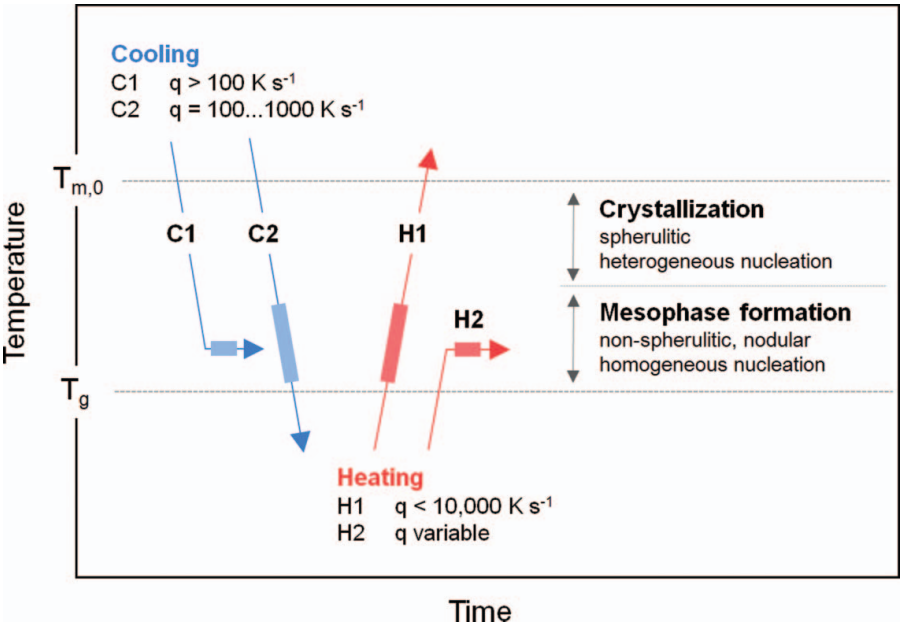

Figure 2. Schematic illustrating the condition of mesophase formation on cooling the quiescent melt (pathways C1 and C2) or heating the amorphous glass (pathways H1 and H2). Adapted from Polymer, Vol. 51, R. Androsch, M.L. Di Lorenzo, C. Schick, B. Wunderlich, "Mesophases in polyethylene, polypropylene, and poly(1-butene)," pages 4639–4662, Copyright 2010, with permission from Elsevier.

formation is passed by continuous heating, the heating rate q must be lower than about 10^4 K s^{-1} (pathway H1).

The temperature ranges of crystallization and mesophase formation are indicated in the right part of Fig. 2. Accordingly, crystallization occurs only between the equilibrium melting temperature and about 330 K; at lower temperature is observed mesophase formation.

Besides analysis of the exact temperature ranges of crystallization and mesophase formation, FSC also allowed evaluation of the overall rates of crystallization and mesophase formation as a function temperature. Crystallization is fastest at temperatures around 350–360 K, while the maximum rate of mesophase formation is observed around ambient temperature [17]. The half-times of crystallization and of mesophase formation at the respective temperatures of fastest growth are about 0.2 and 0.1 s [17]. It is important to note that crystallization and mesophase formation obey qualitatively different kinetics, i.e., a bimodal temperature-dependence of the overall rate of ordering has been observed. The temperature-dependence of the rate of monoclinic crystallization seems to be in accord with the classical crystallization theory [21]. With increasing supercooling, the crystallization rate first increases due to the lowering of the activation energy for creation of a nucleus of critical size, and then it decreases due to lowered mobility of molecule segments. A reason for the bimodal overall rate of crystallization/mesophase formation may be the change of the nucleation mechanism from heterogeneous nucleation at high temperature to homogeneous nucleation at low temperature. Homogeneous nucleation in the temperature range of mesophase formation may overcome the decreasing crystallization rate due to the decreasing mobility of molecular segments, and ultimately causes a repeated increase of

the rate of ordering with decreasing temperature. The frequent homogeneous nucleation, however, does not allow a distinct growth of ordered entities and, correspondingly, the mesophase is reduced in lateral size and of nodular shape.

Both crystallization and mesophase formation in iPP are connected with the development of a distinct rigid amorphous fraction (RAF) at the interface between the ordered phase and amorphous structure [22,23]. The RAF has been detected in partially ordered iPP by quantitative analysis of the heat capacity increment at the glass transition temperature of the mobile amorphous fraction (MAF) ($T_{g,\,MAF}$) at about 260–270 K on its devitrification. Though formation of a RAF seems typical for the majority of crystallizable polymers, in iPP it plays a major role on the crystallization behavior. In quenched samples of iPP of close to 40% mesophase fraction, almost no increase of the heat capacity at $T_{g,\,MAF}$ was observed which suggested that the mesophase coexists at ambient temperature with RAF, and only little MAF. This led also to the conclusion that the mesophase itself was below its own glass transition temperature, i.e., it has been classified as conformationally disordered glass [11].

Reorganization of Semimesomorphic Isotactic Polypropylene

The mesophase of iPP obtained by quenching is metastable at ambient temperature. Increasing temperature leads to perfection of the mesophase [24] and ultimately to conversion into monoclinic crystals. The mesophase—crystal transition involves the removal of intramolecular helix reversal defects and improvement in crystal symmetry, and starts at about 350–360 K with the onset of helix mobility [13,25]. The perfection of the mesophase has been identified by controlled generation of annealing peaks in calorimetric analyses [11,26], and the mesophase—crystal transition has directly been monitored by temperature-resolved X-ray scattering [27,28], as shown in Fig. 3, or by calorimetry [13,24,29]. The latter method also allowed estimation of the rather low specific heat of mesophase ordering of 600 J mol^{-1} [11]. The mesophase—crystal phase transformation is thermodynamically

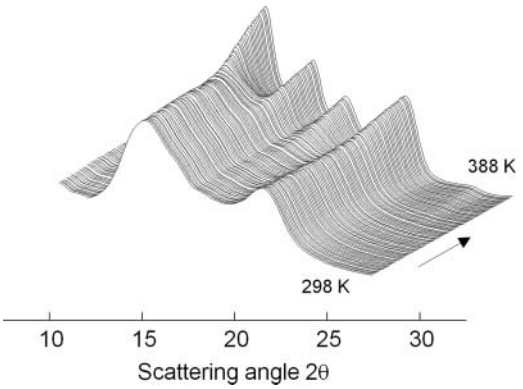

Figure 3. Temperature-resolved X-ray scattering for analysis of the mesophase—crystal phase transition in iPP. Semimesomorphic iPP has been heated from 298 K to 388 K at a rate of 2 K min^{-1}. The X-ray data show the conversion of mesophase into crystals at a temperature of about 350 K—the two characteristic mesophase halos are replaced by sharp peaks characteristic of the monoclinic crystal polymorph. Data were collected at Hasylab. 2010.

irreversible, i.e., subsequent cooling, regardless the cooling rate, does not lead to repeated mesophase transformation.

The reorganization of the mesophase into crystals is kinetically controlled and depends therefore on the heating rate applied. For demonstration, in Fig. 4 is shown a series of FSC heating scans recorded between 5×10^2 K s^{-1} (top curve) and 4×10^4 K s^{-1} (bottom curve) [29]. Samples were initially quenched into the glassy state using a cooling rate of 1×10^4 K s^{-1} according path C2 in Figure 2 and then heated to 300 K for a period of 30 s to allow mesophase formation. Subsequently, the semimesomorphic iPP samples were re-cooled to 100 K, and analyzed by heating at different rates. The endothermic peak labeled I is due to disordering of mesophase formed at 300 K, while the peak labeled III is related to melting of crystals which developed by reorganization of the initially formed mesophase in the temperature range marked II. Increasing heating rate leads to a slight increase of the temperature of disordering and, more important, to an increase of the peak area of event I. Simultaneously the large melting peak III shifts to lower temperature, and decreases in latent heat. On heating at (3–4) $\times$ 10^4 K s^{-1}, finally, only peak I is detected which is related to isotropization of the mesophase without prior perfection and reorganization into crystals (red curves). Note that samples in FSC analyses exhibit micrometer dimensions and a mass of as low as few nanograms, necessary to minimize thermal lags and gradients within the sample. The optical micrograph in Fig. 4 shows a typical FSC sample with a lateral dimension of about 50 μm.

The reorganization of semimesomorphic iPP on heating has also been followed by analysis of the morphology of the ordered phase, using AFM and POM [13,19,30,31]. Most important, it has been found that the mesophase–crystal phase transition has no effect on the size and habit of the nodular mesomorphic domains. This, ultimately, led to the conclusion that the reorganization of the mesophase occurs at local scale within the ordered

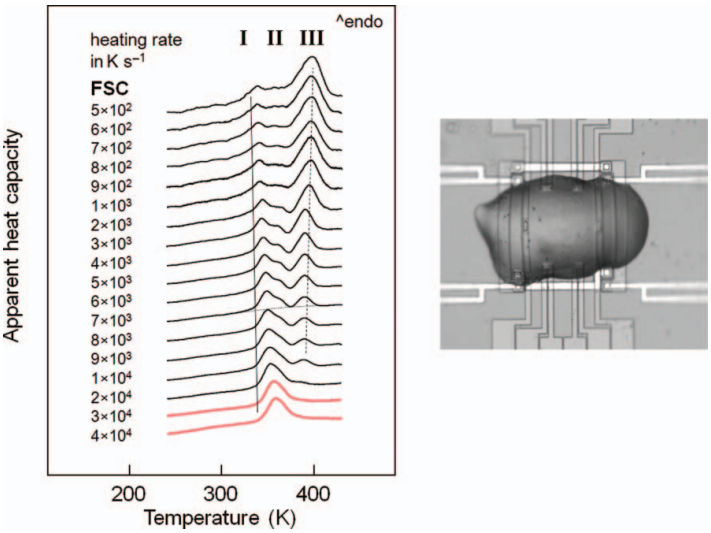

Figure 4. Fast scanning calorimetry (FSC) for analysis of the reorganization behavior of semimesomorphic iPP. Left graph adapted with permission from [29]. Reprinted with permission from D. Mileva, R. Androsch, E. Zhuravlev, C. Schick, Macromolecules, 42, 7275–7278. Copyright 2009 American Chemical Society. The micrograph serves for illustration of the extremely small size of FSC samples, which is of the order of 50 μm in lateral direction.

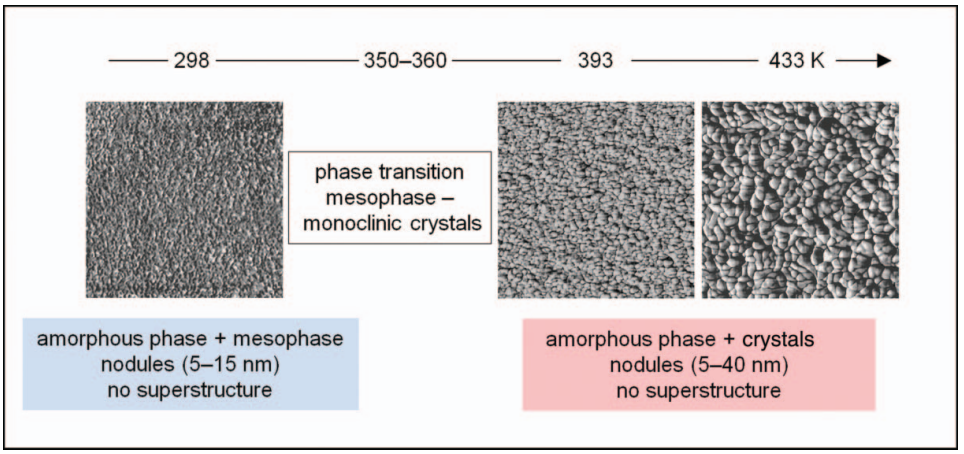

Figure 5. AFM structure of semimesomorphic (left image) and reorganized semicrystalline iPP (center and right images). Reorganization of initially quenched, semimesomorphic iPP was triggered by heating to 393 or 433 K, i.e., to temperatures well above the mesophase—crystal phase transition. The images demonstrate that the mesophase—crystal phase transition does not affect the morphology (size and shape) of the ordered phase. Images adapted from Polymer, Vol. 48, Q. Zia, H.-J. Radusch, R. Androsch, "Direct analysis of annealing of nodular crystals in isotactic polypropylene by atomic force microscopy, and its correlation with calorimetric data", pages 3504–3511, Copyright 2007, with permission from Elsevier.

phase without prior global isotropization of the mesophase. In Fig. 5 are shown AFM images which were collected at ambient temperature on initially semimesomorphic iPP before and after annealing at 393 and 433 K. Before annealing, nodules with a size of about 5–15 nm are observed (left image). Annealing at 393 K, i.e., at a temperature higher than the mesophase—crystal transition, apparently did not result in a change of the size and shape of the ordered, presumably crystalline phase. Only further increase of the temperature led to an increase of the size of nodular crystals by classical annealing processes, to achieve higher stability, with the specific processes described in text books [32]. The final size of crystalline nodules depends on both the maximum annealing temperature and the annealing time, and may reach values of 30 to 40 nm.

Reorganization of semimesomorphic iPP on heating has no effect on the higher-order organization of the ordered phase. Quenching leads to formation of quasi-isometric mesomorphic domains which irregularly are embedded in the amorphous matrix. It has been demonstrated in Figure 1d that the structure is non-spherulitic though heterogeneous. Reorganization of the mesophase into crystals and classical annealing processes do not result in formation of spherulites. In other words, the reorganization of semimesomorphic iPP leads to semicrystalline but non-spherulitic samples, with the crystallinity being at similar level as in case of direct melt-crystallization.

Impact of Crystallization of iPP via the Mesophase

Crystallization of iPP via quenching and formation of a metastable mesophase at ambient temperature in a first step, and subsequent heating to allow mesophase reorganization into crystals permits generation of structures with specific properties which qualitatively are different from those of semicrystalline iPP prepared by direct melt-crystallization.

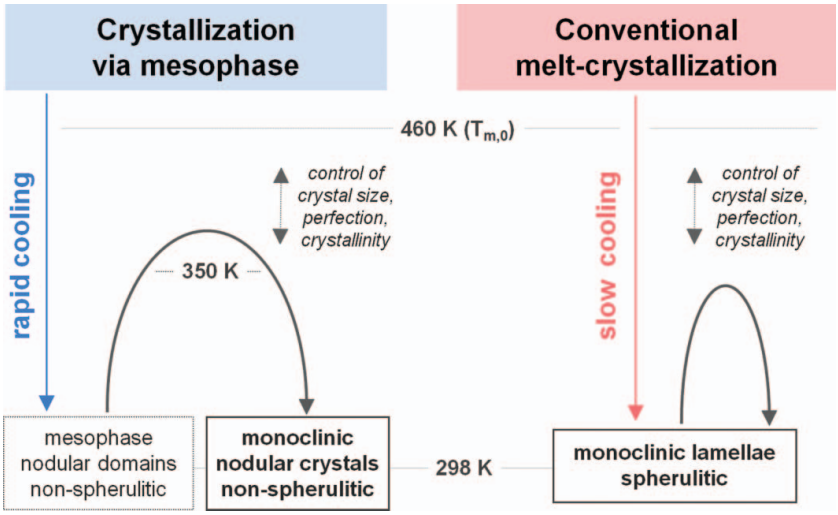

Figure 6. Schematic of different pathways of crystallization the quiescent melt of iPP: Crystallization via the mesophase (left) and conventional, direct crystallization of the melt (right). Based on a sketch published in [33]. With kind permission from Springer Science+Business Media: Polymer Bulletin, Deformation behavior of isotactic polypropylene crystallized via a mesophase, Vol. 63, 2009, pages 755–771, Q. Zia, H.-J. Radusch, R. Androsch, Fig. 1.

Figure 6 is a sketch of different pathways of crystallization of the quiescent melt of iPP, and summarizes essential steps to obtain different supermolecular semicrystalline structures of iPP [33]. Crystallization via the mesophase (left) requires quenching at a rate faster than 10^2 K s^{-1} to room temperature, to obtain a mesophase of nodular geometry in a non-spherulitic environment, and subsequent annealing at a temperature higher than about 350 K. The annealing step triggers mesophase reorganization into monoclinic crystals, with the annealing temperature and time controlling structural parameters, like the nodule size, the internal perfection of crystals and the crystallinity. Finally, a semicrystalline iPP is obtained with spatially non-organized nodular monoclinic crystals. Conventional melt-crystallization (right) includes slow cooling of the quiescent melt at a rate lower than 10^2 K s^{-1} which leads to direct conversion of liquid into monoclinic crystals of lamellar shape, organized within spherulites. Similar as in case of crystallization via the mesophase, subsequent annealing allows again control of the lamellar thickness, or of the crystallinity.

Figures 7 and 8 compare the tensile stress—strain behavior and the optical transparency of semicrystalline iPP prepared by different pathways of crystallization, as explained with Fig. 6. Qualitatively, the data of Fig. 7 reveal that conventional melt-crystallization, accompanied by formation of lamellae and of spherulites, leads to rather non-ductile samples. Failure is observed immediately on passing the yield point (see e.g. the curve marked by the red shaded numeral). In contrast, crystallization via the mesophase leads to samples which show ductile deformation behavior (see e.g. the curve marked by the blue shaded numeral). Using each preparation scheme, three samples of different crystallinity have been prepared. The crystallinity is proportional to the density given in the legend of Fig. 7. As expected, the yield stress and the modulus of elasticity increase with the crystallinity/density. Most important, the curves labeled '3' exhibit identical crystallinity, however, show largely different tensile stress—strain behavior. Young's modulus of these two samples is almost identical.

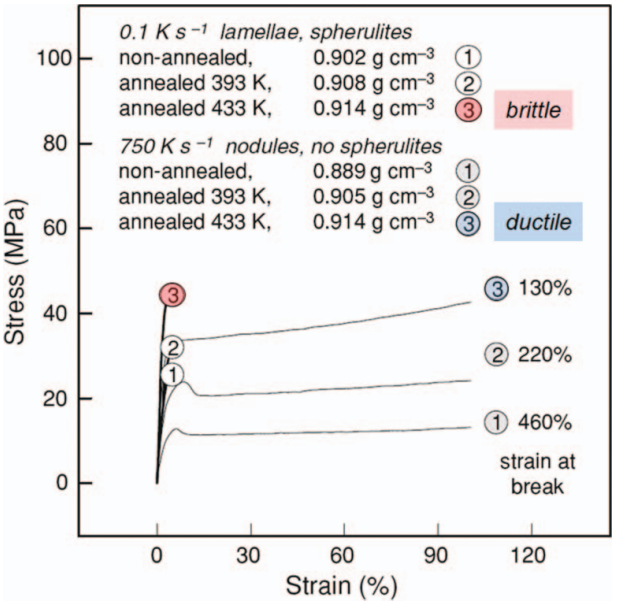

Figure 7. Tensile stress—strain behavior of conventionally crystallized iPP (bold lines, failure at yield point), and of iPP crystallized via the mesophase (thin lines, strain at break >100%). Note, the curves labeled '3' exhibit identical crystallinity/density but show largely different large-strain behavior/ductility. With kind permission from Springer Science+Business Media: Polymer Bulletin, Deformation behavior of isotactic polypropylene crystallized via a mesophase, Vol. 63, 2009, pages 755–771, Q. Zia, H.-J. Radusch, R. Androsch, Fig. 2.

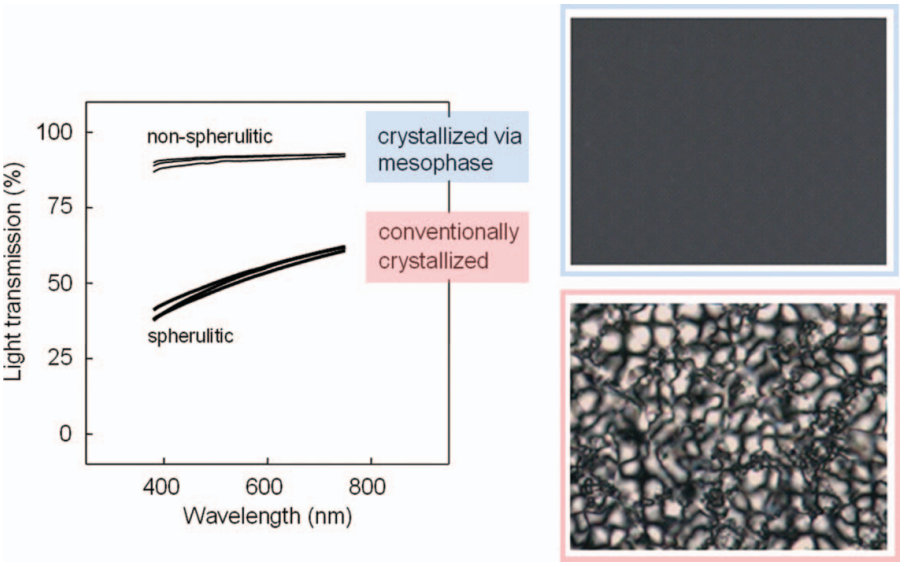

Figure 8. Light transmission of conventionally crystallized, spherulitic iPP, and of non-spherulitic iPP crystallized via the mesophase as a function of the wavelength. Adapted with kind permission from [33]. Copyright 2010, John Wiley and Sons.

In first approximation, we assume that the modulus of elasticity mainly is controlled by the crystallinity and intra- and intermolecular forces at segment level, and to lesser degree by the morphology of crystals or even the superstructure. The latter, i.e., the crystal shape, their mutual orientation/cross-hatching and the superstructure, however, control the large-strain behavior, including rotation and dissolution of lamellae, before final formation of micro-fibrils.

In Fig. 8 is demonstrated the effect of presence of spherulites on the transmission of visible light through films of 100 μm thickness in semicrystalline preparations of iPP. Absence of spherulites, as is achieved by crystallization via the mesophase leads to optically highly transparent films with the light transmission exceeding 90–95%. Spherulitic samples of identical crystallinity, in contrast, are rather opaque and the light transmission is about only 50%. The reasons for the different optical behavior of spherulitic and non-spherulitic samples have been described in detail in a separate study [34].

Regarding properties of iPP, it can be summarized that highly transparent films (controlled by absence of spherulites) of high Young's modulus (controlled by the crystallinity), and high ductility (controlled by absence of both spherulites and non-isometric lamellar crystals) can be observed by crystallization via the mesophase. Classical melt-crystallization by direct conversion of liquid into crystals also leads to samples of high Young's modulus; however, the optical transparency and ductility are strongly reduced by the presence of spherulites.

Acknowledgments

The research has partially been funded by the Deutsche Forschungsgemeinschaft (DFG) (DM, RA) and the European Union (CS, EZ). The authors furthermore acknowledge financial support by DESY.

References

[1] Pasquini, N. (2005). *Polypropylene Handbook*, Carl Hanser Verlag: Munich, Germany.
[2] Natta, G., & Corradini, P. (1960). *Nuovo Cimento Suppl*., *15*, 40.
[3] Natta, G. (1960). *Makromol. Chem.*, *35*, 94.
[4] Addink, E. J., & Beintema, J. (1961). *Polymer*, *2*, 185.
[5] Turner-Jones, A., Aizlewood, J. M., & Beckett, D. R. (1964). *Makromol. Chem.*, *75*, 134.
[6] Binsbergen, F. L., & De Lange, B. G. M. (1968). *Polymer*, *9*, 23.
[7] Hsu, C. C., Geil, P. H., Miyaji, H., & Asai, K. (1986). *J. Polym. Sci., Polym. Phys.*, *24*, 2379.
[8] Ogawa, T., Miyaji, H., & Asai, K. (1985). *J. Phys. Soc. Jpn., Letters*, *54*, 3668.
[9] Lotz, B., Wittmann, J. C., & Lovinger, A. J. (1996). *Polymer*, *37*, 4979.
[10] Wunderlich, B., & Grebowicz, J. (1984). *Adv. Polym. Sci.*, *60/61*, 1.
[11] Grebowicz, J., Lau, S.-F., & Wunderlich, B. (1984). *J. Polym. Sci., Symp.*, *71*, 19.
[12] Mileva, D., Zia, Q., Androsch, R., Radusch, H.-J., & Piccarolo, S. (2009). *Polymer*, *50*, 5482.
[13] Androsch, R., Di Lorenzo, M. L., Schick, C., & Wunderlich, B. (2010). *Polymer*, *51*, 4639.
[14] Wu, Z. Q., Dann, V. L., Cheng, S. Z. D., & Wunderlich, B. (1988). *J. Therm. Anal.*, *34*, 105.
[15] De Santis, F., Adamovsky, S., Titomanlio, G., & Schick, C. (2006). *Macromolecules*, *39*, 2562.
[16] Gradys, A., Sajkiewicz, P., Minakov, A. A., Adamovsky, S., Schick, C., Hashimoto T., & Saijo, K. (2005). *Mat. Sci. Eng.*, *A413–A414*, 442.
[17] Silvestre, C., Cimmino, S., Duraccio, D., & Schick, C. (2007). *Macromol. Rap. Comm.*, *28*, 875.
[18] Piccarolo, S. (1992). *J. Macromol. Sci., Phys.*, *B31*, 501.
[19] Zia, Q., Androsch, R., Radusch, H.-J., & Piccarolo, S. (2006). *Polymer*, *47*, 8163.
[20] The ATHAS Data Bank of the thermodynamic functions and glass transition temperatures of polymers. (http://athas.prz.rzeszow.pl.)

[21] Hoffmann, J. D., Davis, G. T., & Lauritzen, J. I. (1976). The rate of crystallization of linear polymers with chain folding. In: H. B. Hannay (Ed.), Treatise on solid state chemistry, crystalline and noncrystalline solids, Vol. 3. New York: Plenum Press.
[22] Wunderlich, B. (2003). *Progr. Polym. Sci.*, *28/3*, 383.
[23] Zia, Q., Mileva, D., & Androsch, R. (2008). *Macromolecules*, *41*, 8095.
[24] Mileva, D., Androsch, R., Zhuravlev, E., Schick, C., & Wunderlich, B. (2011). *Thermochim. Acta*, *522*, 100.
[25] Schaefer, D., Spiess, H. W., Suter, U. W., & Fleming, W. W. (1990). *Macromolecules*, *23*, 3431.
[26] Fichera, A., & Zannetti, R. (1975). *Makromol. Chem.*, *176*, 1855.
[27] Wang, Z. G., Hsiao, B. S., Srinivas, S., Brown, G. M., Tsou, A. H., Cheng, S. Z. D., & Stein, R. S. (2001). *Polymer*, *42*, 7561.
[28] O'Kane, W. J., Young, R. J., Ryan, A. J., Bras, W., Derbyshire, G. E., & Mant, G. R. (1994). *Polymer*, *35*, 1352.
[29] Mileva, D., Androsch, R., Zhuravlev, E., & Schick, C. (2009). *Macromolecules*, *42*, 7275.
[30] Zia, Q., Radusch, H.-J., & Androsch, R. (2007). *Polymer*, *48*, 3504.
[31] Androsch, R. (2008). *Macromolecules*, *41*, 531.
[32] Wunderlich, B. (1976). *Macromolecular Physics, 2, Crystal nucleation, Growth, Annealing*, Academic Press: New York, USA.
[33] Zia, Q., Radusch, H.-J., & Androsch, R. (2009). *Polym. Bull.*, *63*, 755.
[34] Zia, Q., Androsch, R., & Radusch, H.-J. (2010). *J. Appl. Polym. Sci.*, *117*, 1013.